WARSAW UNIVERSITY OF TECHNOLOGY Index 351733
FACULTY OF CIVIL ENGINEERING
COMMITTEE FOR CIVIL AND WATER ENGINEERING
POLISH ACADEMY OF SCIENCES ISSN 1230-2945

DOI: 10.24425/ace.2026.1412

ARCHIVES OF CIVIL ENGINEERING

Vol. LXXII ISSUE 3 2026

 pp. 525 – 540

Research paper

Pore pressure and stiffness characteristics of artificial freeze-thaw soft soil under bidirectional cyclic load

Bowen Kong[1], Hao Jiang[2], Huan He[3], Yuntian Yan[4], Baoping Zou[5]

Abstract: To explore the mechanism of uneven settlement of the cross-river subway under bidirectional cyclic load after the artificial ground freezing method, this paper analyzes the pore pressure and stiffness of saturated soft clay in Hangzhou. A dynamic triaxial apparatus was used to conduct cyclic loading tests on the reshaped silt soft soil after freezing and thawing, and the evolution patterns of pore pressure and stiffness in relation to cyclic loading cycles were quantified. The test results show that: freezing action damages the soil microstructure, and the pore pressure development level of frozen soil is higher than that of unfrozen soil; when the dynamic stress level is less than a certain value, the stiffness of silty soft soil shows a hardening trend under cyclic loading; With the soil consolidation confining pressure and radial cyclic stress ratio increases, the pore pressure stability value increases, and the increase in soil stiffness increases also. Based on the test results, a prediction model, considering the ratio of effective confining pressure to radial cyclic stress, for the development of pore water pressure in freeze-thaw soft soil under bidirectional cyclic loading is established. The study found that as the soil skeleton structure is compacted, the soil pore pressure stability value and stiffness increase. And within the range of stiffness hardening, the pore pressure stability value and stiffness increase are linearly related.

Keywords: artificial ground freezing, bidirectional cyclic load, pore pressure prediction model, stiffness, dynamic characteristics, dynamic triaxial

[1]PhD., School of Civil Engineering and Architecture, Zhejiang University of Science and Technology, Zhejiang 310023, China, e-mail: kbw@zust.edu.cn, ORCID: 0000-0002-1369-0616
[2]MSc., School of Civil Engineering and Architecture, Zhejiang University of Science and Technology, Zhejiang 310023, China, e-mail: h1509195629@163.com, ORCID: 0009-0008-3666-5692
[3]MSc., School of Civil Engineering and Architecture, Zhejiang University of Science and Technology, Zhejiang 310023, China, e-mail: hehuan465@163.com, ORCID: 0009-0002-8843-2184
[4]MSc., School of Civil Engineering and Architecture, Zhejiang University of Science and Technology, Zhejiang 310023, China, e-mail: yanyuntian1013@163.com, ORCID: 0009-0003-5151-2794
[5]PhD., School of Civil Engineering and Architecture, Zhejiang University of Science and Technology, Zhejiang 310023, China, e-mail: zoubp@zust.edu.cn, ORCID: 0000-0003-3729-2425

1. Introduction

The artificial ground freezing technique is widely utilized in the construction of tunnels in areas with soft soil, particularly in China's Yangtze River Delta [1]. Nonetheless, the dynamic characteristics of soft soils are significantly reduced over repeated cycles of freezing and thawing [2, 3]. Microstructurally, the expansion of ice crystals during freezing disrupts soil particle arrangements, creating microcracks and weakening interparticle cementation, while subsequent thawing further destabilizes the skeletal framework by redistributing unfrozen water into enlarged pores. Temperature variations during freezing, which induce uneven settlement in frozen areas, pose significant operational risks to subway systems [4]. As a result, it is required to analyze the phenomena of uneven settlement in subway system submerged foundations under the effect of train loads during the operating period following the application of the artificial freezing approach. This study is critical for ensuring the safety and dependability of subway developments.

Hangzhou subway pipes over the Qiantang River must not only handle subway traffic but also the Qiantang River's tidal load [5]. According to Jie Zhou and Yiqun Tang [6], the residual cumulative plastic strain of soft clay following artificial freeze-thaw under subway low-level cyclic stress appears to exhibit asymptotic behavior, starting off quickly and then slowing down to achieve a steady value. Furong Liu, Zhiwei Zhou et al. [7] discovered that a significant role in permafrost deformation is the direction of major stresses in the subgrade soil under cyclic loading. Yang Yugui et al. [8] demonstrated that strain softening was observed in artificial permafrost during shear, whereas strain hardening dominated at higher confining pressures; however, as perimeter pressure increased, strain softening reduced and strain hardening occurred at high perimeter pressure. Water content and perimeter pressure influence the strength of artificial permafrost. The strength of low water content artificial permafrost always grows as the perimeter pressure increases; whereas, the strength of high water content artificial permafrost increases and then falls as the perimeter pressure increases. Established research have demonstrated that the rate of rise in pore water pressure amplitude is accelerated and the pore water pressure stability value is raised [9–11]. Zhong Zuliang et al. [12] employed the cyclic load dynamic triaxial test to investigate the impacts of early consolidation, effective consolidation confining pressure, and soil softening. Additionally, the stiffness softening level beneath the dynamic level of the real train load is difficult to attain when the tunnel burial depth is deep, and the development law of the hardening of soft soil stiffness has not been completely researched. The dynamic properties of soil, including pore pressure and stiffness, are significantly influenced by additional horizontal cyclic stress. However, most existing research focuses on unfrozen soils, leaving the coupled effects of freeze-thaw cycles and bidirectional loading on soft clays underexplored, not involved in the construction of the subway after the artificial freezing method of the tunnel across the river, to explore the mechanism of the change is slow.

This study aims to explore the effects of varying confining pressure and radial cyclic stress ratio on the pore pressure and stiffness of freeze- thawed soils under bidirectional cyclic loading. After remolding and equivalent freeze-thaw treatment, saturated clay samples were tested under bidirectional cyclic loading using a GDS triaxial instrument. The tests analyzed the impacts of confining pressure and radial cyclic stress ratio on pore pressure and stiffness.

Results showed a linear link between pore pressure limits and soil stiffness gain. A predictive model for pore pressure evolution in freeze-thawed soils, considering the ratio of effective confining pressure to radial cyclic stress, was also proposed.

2. Test equipment, materials and methods

2.1. Test equipment

The dynamic characterization test uses GDS's servo-motor-based bidirectional dynamic triaxial system (as shown in Fig. 1). It assesses soil dynamic parameters like stress, strain, and pore pressure. Water is the loading medium, with the servo system motor adjusting piston movement to apply pressure. GDSLAB software ensures effective control and data collection per vibration cycle. Dynamic triaxial tests with a GDS triaxial device ensure accurate pore pressure and stiffness measurement. Soil sample preparation steps are as follows.

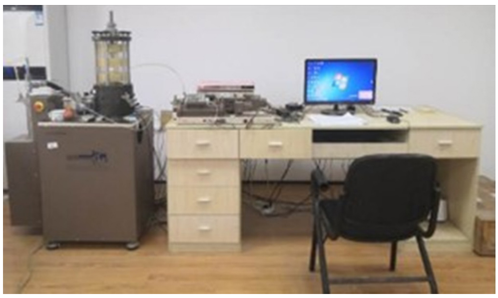

Fig. 1. GDS dynamic triaxial instrument

2.2. Selection and preparation of soil samples

The test material is silty saturated soft clay from 15–20 m depth near a Hangzhou subway station foundation pit. The soil sample, dominated by illite and illite-montmorillonite minerals, exhibits low strength, low permeability, high compressibility, and high sensitivity. The saturated soft clay has a natural weight of 17.7 kN/m^3, density $\rho = 1.82$ g/cm^3, relative density $G_s = 2.75$, water content $w = 45\%$, plastic limit $w_p = 33.4\%$, liquid limit $w_L = 51.6\%$, and plasticity index $I_p = 18.2$, and the test employed the vacuum precompression method to avoid errors caused by poor homogeneity in original soil, producing remolded soil samples with enhanced uniformity [2].

Before the experiments, soil samples were prepared for dynamic triaxial testing by vertically cutting remolded soil with a sampler (Fig. 2). The samples were placed in a saturator with porous stones at both ends and pre-saturated in a vacuum chamber. Following geotechnical test standards (SL37-1999), vacuum saturation involved 3 hours at –0.1 MPa followed by 12 hours of atmospheric-pressure immersion.

Fig. 2. Cut the specimen

2.3. Test parameters

Dynamic triaxial tests involve sample installation, saturation, consolidation, and loading. The saturated sample is sealed in a pressure chamber with a rubber membrane, followed by backpressure saturation (20 kPa differential pressure). Saturation is confirmed when the degree exceeds 0.97 for 10 minutes. Isotropic consolidation is performed under effective confining pressure, followed by undrained cyclic loading via the GDSLAB program with predefined patterns, frequency, and cycles.

This study conducted dynamic triaxial tests on freeze-thawed soil samples using biased sinusoidal cyclic loading. Based on Hangzhou subway tunnel burial depth measurements [1], parameters included 30 kPa axial static bias stress, 20 kPa cyclic loading amplitude, and 1 Hz frequency. The cross-river subway loading incorporates horizontal and axial vibration components [13]. Axial vibration was applied through the top seat, while horizontal cyclic stress (1 Hz biased sinusoidal waveform) was independently controlled by the perimeter pressure system [14]. Specimens experienced compressive stresses only, consistent with subway-induced soil stress paths (Fig. 3).

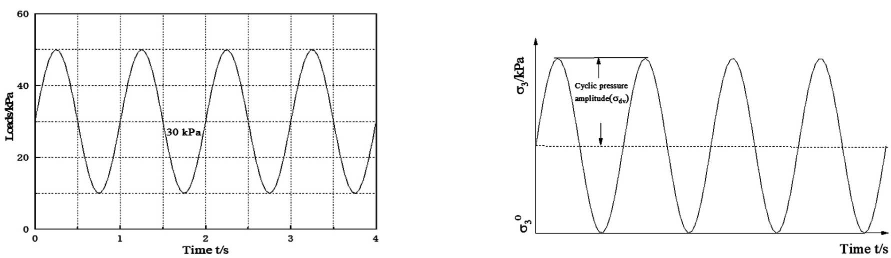

(a) (b)

Fig. 3. Load waveform; (a) Axial load, (b) Horizontal directional load

All of the freeze-thaw soil samples used in this study were frozen at –20°C for 24 hours before being thawed at room temperature at 25°C for 24 hours. Fig. 4 displays the soil samples after freezing. The soil samples' surface developed a network of fissures after freezing.

Fig. 4. Soil samples after freezing

The axial cyclic pressure amplitude is denoted as σ_{dr}, the horizontal cyclic stress ratio is denoted as σ_{dv}, and their ratio is defined as the radial cyclic stress ratio $\tau_r = \sigma_{dr}/\sigma_{dv}$. This chapter applies radial cyclic stress ratios of 0, 0.2, 0.5, and 1 to artificial freeze-thawed soil, determining horizontal stress amplitudes accordingly. Each 10-meter increase in overburden soil thickness corresponds to a 100 kPa effective confining pressure increment. For the Hangzhou cross-river subway tunnel, the effective confining pressure ranges from 150 to 250 kPa. The test program is presented in Table 2. Test plan, wherein q_s represents the initial static bias stress, T denotes the freezing temperature, f signifies the vibration frequency, p' represents the confining pressure during the loading phase, and N denotes the number of cyclic loading.

Table 1. Test plan

Specimen number	q_s/kPa	τ_r/kPa	T/°C	f/Hz	p'/kPa	N
T1	30	0	–20	1	250	20000
T2	30	0	–20	1	200	20000
T3	30	0	–20	1	150	20000
T4	30	0.2	–20	1	250	20000
T5	30	0.2	–20	1	200	20000
T6	30	0.2	–20	1	150	20000
T7	30	0.5	–20	1	250	20000
T8	30	0.5	–20	1	200	20000
T9	30	0.5	–20	1	150	20000
T11	30	1	–20	1	250	20000
T12	30	1	–20	1	200	20000
T13	30	1	–20	1	150	20000

3. Study on the pore pressure characteristics

3.1. Test parameters

Under vibratory loading, soil pore pressure exhibits cyclic fluctuations (Fig. 3a). Unidirectional loading shows initial amplitude is around 2 kPa with 1-2 kPa residual accumulation per cycle, while bidirectional loading (Fig. 5 Pore pressure changes at the beginning of loading b) reaches 20 kPa amplitude with negligible initial residual accumulation.

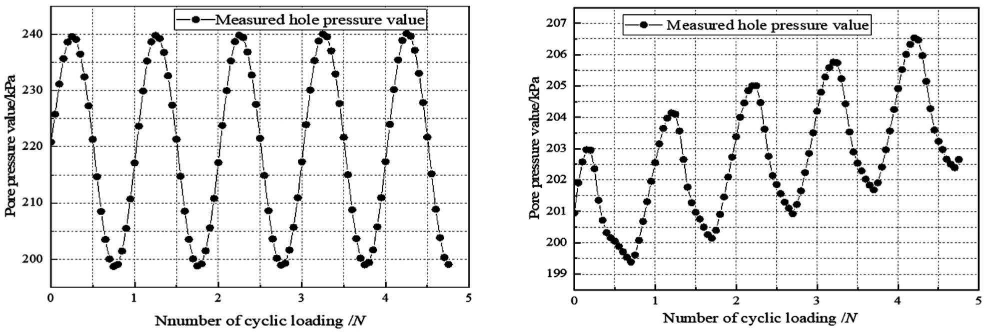

(a) (b)

Fig. 5. Pore pressure changes at the beginning of loading; (a) Unidirectional loading, (b) Bidirectional loading

Pore pressure evolution differs significantly between unidirectional and bidirectional loading. Under bidirectional conditions, cyclic confining pressure masks residual pore pressure accumulation from axial loading, as their synchronized frequency and phase alignment amplifies the dominance of cyclic confining pressure effects on pore pressure development.

3.2. Effect of freezing on the development of pore pressure

Dynamic tests on freeze-thawed soft soil using stress-controlled biased sinusoidal loading revealed cyclic pore pressure fluctuations. Fig. 6(a)–6(f) compare cumulative residual pore pressure increments between unfrozen soil [5] and freeze-thawed soil under identical conditions with varying radial cyclic stress ratios. All curves exhibited three-phase growth: rapid growth, steady growth, and equilibrium. Initial cycles showed minimal soil skeleton deformation with pore water bearing loads, while subsequent cycles demonstrated reduced residual pressure growth rates as the skeleton stabilized. The equilibrium-phase pressure was defined as the pore pressure limit.

As shown in Fig. 6(a) and 6(b), freeze-thawed soils exhibit higher cumulative pore pressure limits than unfrozen soils under varying radial stress ratios, attributed to ice-induced microcracks enhancing pore water migration. Their stabilized residual pore pressures are 3–5 kPa higher, with delayed pore pressure stabilization under prolonged cyclic loading.

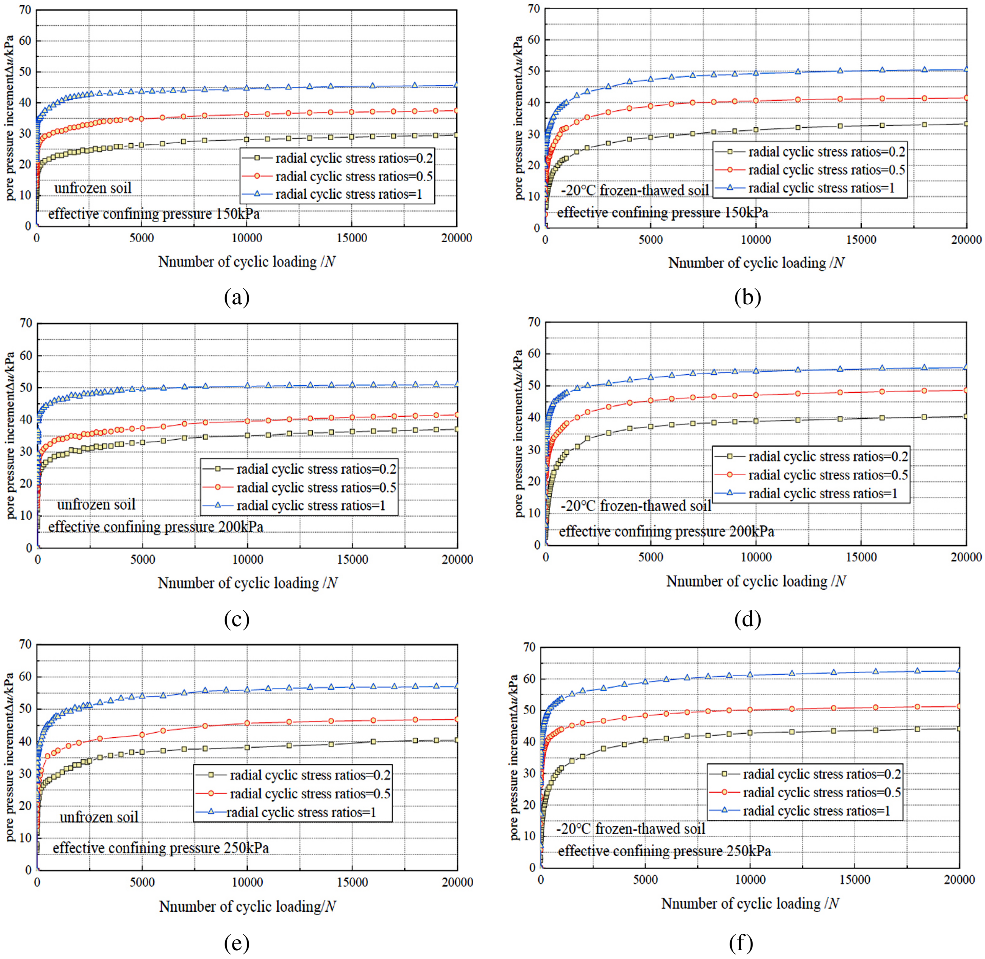

Fig. 6. Development of pore pressure in frozen soil and unfrozen soil under bidirectional cyclic loading; (a) Unfrozen soil, 150 kPa, (b) Frozen-thawed soil, 150 kPa, a) Unfrozen soil, 200 kPa, (b) Frozen-thawed soil, 200 kPa, a) Unfrozen soil, 250 kPa, (b) Frozen-thawed soil, 250 kPa

3.3. Development of pore pressure in freeze-thawing soft soil under different load conditions

The cross-river subway's 7–15 m overburden heightens residual pore pressure under increased effective confining pressure, with dissipation exacerbating soil settlement. Fig. 7 shows cumulative pore pressure curves under unidirectional and bidirectional loading. At 100-150 kPa confining pressure, additional horizontal cyclic loading increases stabilized pore pressure by 7–10 kPa, while at 250 kPa the increase is below 5 kPa, demonstrating that higher effective confining pressure reduces pore pressure sensitivity to comparable horizontal loading.

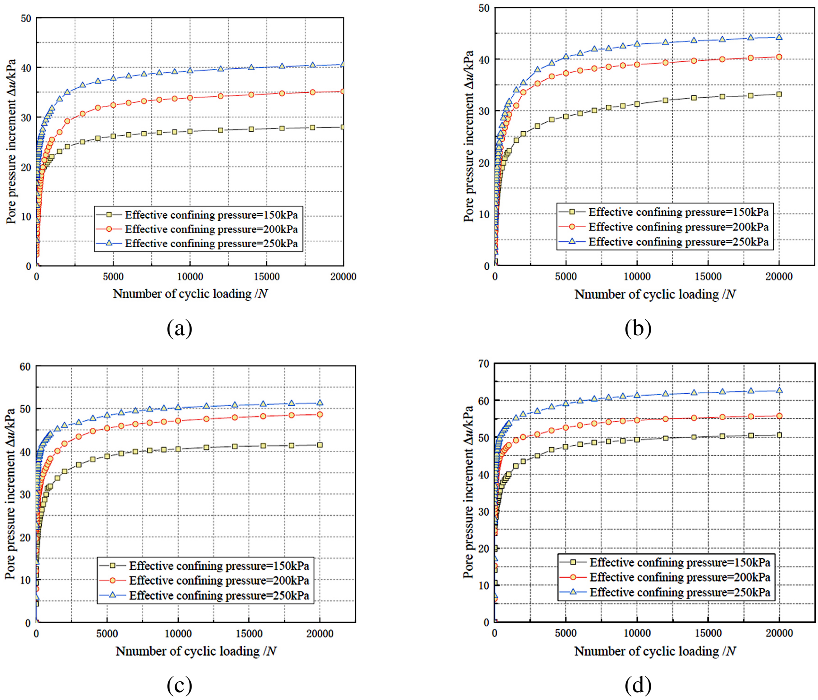

Fig. 7. Effect of effective confining pressure on the development of pore pressure in freeze-thaw soil; (a) Radial cyclic stress ratio = 0, (b) Radial cyclic stress ratio= 0.2, (c) Radial cyclic stress ratio = 0.5, (d) Radial cyclic stress ratio = 1

The pore pressure stability value rises with increasing confining pressure. When effective confining pressure rises from 150 kPa to 250 kPa, the stability value increases by about 15–20 kPa, with each 50 kPa confining pressure increment causing a 5–7 kPa stability value rise. Under a radial cyclic stress ratio of 1, unidirectional loading raises the stability value from 25 kPa to 40 kPa, while bidirectional loading raises it from 45 kPa to 64 kPa. This indicates that during bidirectional loading, residual pore pressure increases with thicker overburden soil, worsening non-uniform settlement.

3.4. The pore pressure prediction model

Existing pore water pressure prediction models, by integrating freeze-thaw damage and bidirectional cyclic loading coupling effects, more accurately characterize pore pressure evolution mechanisms in freeze-thawed soft soils under complex stress conditions compared to conventional models. Researchers have developed various cumulative pore pressure prediction models based on specific test conditions, including the first-order logarithmic model proposed by Zhou Jian [16], the exponential model established by Ye Junneng et al. [17], and the quadratic logarithmic model proposed by Ding Zhi et al. [18]. Extensive studies have investigated the influences of drainage parameters, soil stress history, and cyclic stress levels on pore pressure development [19]. Current research shows limited exploration of pore pressure in silty soft soils under different radial cyclic stress ratios and confining pressure combinations, with a notable gap in modeling pore pressure development under bidirectional loading after freeze-thaw cycles. Developing a predictive model that accurately reflects excess pore pressure growth in silty soft soils induced by subway cyclic loading is crucial for simulating pore pressure evolution in real engineering scenarios and predicting soil settlement under cyclic loading conditions.

$$r_u = A \cdot \left(\frac{p}{p_0}\right)^2 \cdot \ln^2(N) + B \cdot \left(\frac{p}{p_0}\right) \cdot \ln(N) + C \cdot a \ \cdot \exp(\tau_r) \tag{3.1}$$

where: r_u is the super pore pressure ratio ($r_u = \Delta u/p$), p is the effective confining pressure, p_0 is the soil consolidation pressure, N is the number of cyclic loading, τ_r is the radial cyclic stress ratio suffered by the soil, α is the damage coefficient related to freezing conditions, and A, B and C are the parameters of the model fitting obtained from the tests. The model achieves faster pore pressure stabilization during bidirectional loading than unidirectional loading due to quicker pore pressure generation. It considers the effects of effective confining pressure and radial cyclic stress ratio on soft clay pore pressure under cyclic loading in cross-river subway projects. Fig. 8 shows the model-experiment fitting results under various effective confining pressures, indicating that the model accurately represents the pore pressure evolution in soft clay under cross-river subway loading and correlates well with experimental findings.

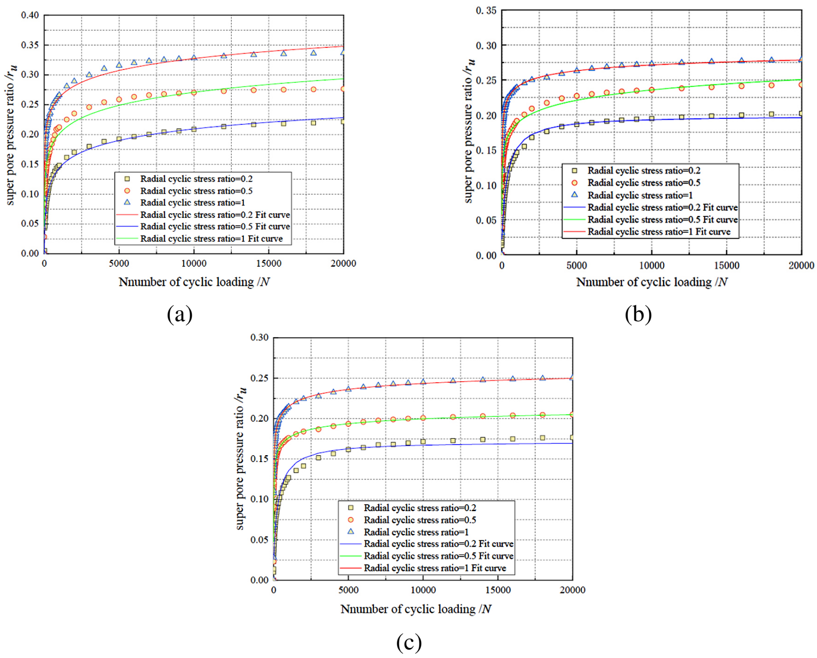

Fig. 8. Pore pressure fitting curves under different radial cyclic stress ratios; (a) Effective confining pressure = 150 kPa, (b) Effective confining pressure = 200 kPa, (c) Effective confining pressure = 250 kPa

Fig. 8. Pore pressure fitting curves under different radial cyclic stress ratios shows that the excess pore pressure ratio increases with radial cyclic stress ratio. At 150 kPa effective confining pressure, raising the radial cyclic stress ratio from 0.2 to 1 elevates the ratio by 136.7% and 107.5%, while at 250 kPa the same stress ratio increments result in only 43.3% and 23.4% increases. Higher effective confining pressure substantially reduces the radial cyclic stress ratio's influence on pore pressure, consistent with Wang Jun's findings for unfrozen silty soft soil under bidirectional loading [20].

The quadratic logarithmic models in Fig. 8. Pore pressure fitting curves under different radial cyclic stress ratios describe pore pressure under different radial cyclic stress ratios, with Table. 2. The fitting parameters showing fitting parameters and goodness of fit exceed 0.98. Compared to unfrozen soil [5], freeze-thawed soil requires more cycles to stabilize pore pressure and exhibits poorer model consistency. This instability likely stems from soil particle disruption caused by ice expansion during freeze-thaw cycles, enhancing deformability and pore pressure instability. Both pore pressure and stiffness characteristics demonstrate the coupled effects of freeze-thaw cycles and bidirectional loading on soil dynamic responses.

Table 2. The fitting parameters

P	Radial cycle stress ratio	A	B	C	degree of fitting
150	0.2	3.27×10^4	0.033	0.073	0.986
150	0.5	8.39×10^4	0.016	0.045	0.984
150	1	4.28×10^4	0.021	0.094	0.991
200	0.2	1.939×10^4	0.010	0.003	0.985
200	0.5	2.214×10^4	0.017	0.057	0.984
200	1	1.398×10^4	0.033	0.064	0.987
250	0.2	7.943×10^4	0.010	0.004	0.983
250	0.5	1.255×10^4	0.030	0.057	0.994
250	1	9.18×10^4	0.024	0.047	0.984

4. Study on stiffness characteristics

4.1. Analysis of stiffness and hardening characteristics

Soil stiffness is determined by the gradient of the hysteresis loop endpoints in stress-strain curves under cyclic loading. Zhang Tao's dynamic triaxial tests on Hangzhou silty clay reveal that stiffness increases under low dynamic stress and decreases under high dynamic stress [21]. This study defines stiffness increase as hardening behavior and decrease as softening behavior.

Tests adopt subway-measured loading data with three stress ratios (0.13, 0.1, 0.08) under effective consolidation stress. Some samples exhibit stiffness softening at low dynamic stress levels (150 kPa confining pressure), aligning with Wei Xinjiang's finding that soil stiffness transitions from hardening to softening as cyclic stress ratio increases [22]. As shown in Fig. 9 for T2 specimens under bidirectional loading, hysteresis loop area reduction, tighter spacing, and lower slope with increasing cyclic loading indicate soil particle densification leading to stiffness hardening.

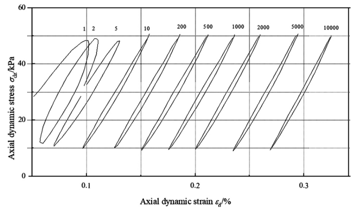

Fig. 9. Hysteresis loop of T2 sample

This study introduces the stiffness hardening concept based on Idriss's stiffness softening theory. The softening index increases with cyclic loading events, reflecting enhanced soil stiffness. The stiffness calculation methodology is as follows:

(4.1)
$$G_N = \frac{q_{\max} - q_{\min}}{\varepsilon_{\max} - \varepsilon_{\min}}$$

(4.2)
$$\delta = G_N / G_{\max}$$

where: GN is the soil stiffness in a cycle, $q_{\max}$ is the maximum bias stress in a cycle, $q_{\min}$ is the minimum bias stress in a cycle, $\varepsilon_{\max}$ is the maximum axial strain in a cycle, $\varepsilon_{\min}$ is the minimum axial strain in a cycle, $G_{\max}$ is the maximum stiffness in a cycle, and δ is the softening index.

Fig. 10 compares soil stiffness variation curves in linear and semi-logarithmic coordinate systems to analyze stiffness changes under different cycle numbers [23]. In the linear system, stiffness increases rapidly within 2000 cycles, slows between 2000–8000 cycles, and stabilizes beyond 8000 cycles. Due to the large cycle range, the semi-logarithmic system better illustrates the relationship between stiffness and cycle number. This section focuses on the stiffness variation pattern under the discussed factors, specifically examining the semi-logarithmic stiffness curve for the first 12000 cycles after data simplification. Given the lack of universality in stiffness model complexity, no stiffness prediction model is established here.

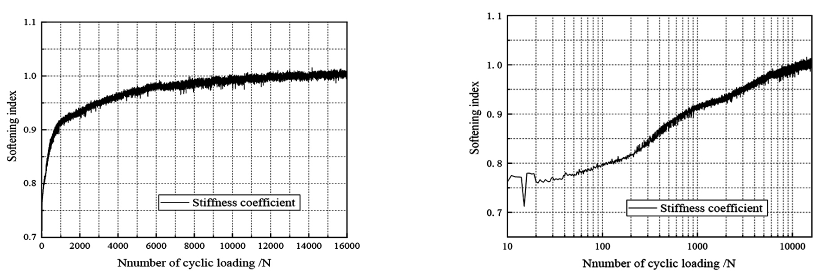

(a) (b)

Fig. 10. Variation of soil sample stiffness in different coordinate systems; (a) Constant coordinate system, (b) Semi-logarithmic coordinate system

4.2. Effect of radial cyclic stress ratio on the stiffness of freeze-thaw soft soil

As shown in Fig. 11, among the studied dynamic stress parameters, only specimens with a radial cyclic stress ratio of 0.2 and effective confining pressure of 150 kPa exhibit stiffness reduction (25% softening index decrease), while others show hardening. Within the hardening range, higher horizontal dynamic confining pressure amplifies variations in the soil softening index. At 200 kPa consolidation confining pressure, increasing the radial stress ratio from 0.2 to 1 reduces the softening index by approximately 14%; at 250 kPa, the reduction is about 10%. Elevated confining pressure diminishes the enhancement of stiffness through radial cyclic stress ratio increases, reducing ultimate soil compactness but improving stiffness. The influence of radial cyclic stress ratio variations on stiffness weakens with rising effective confining pressure.

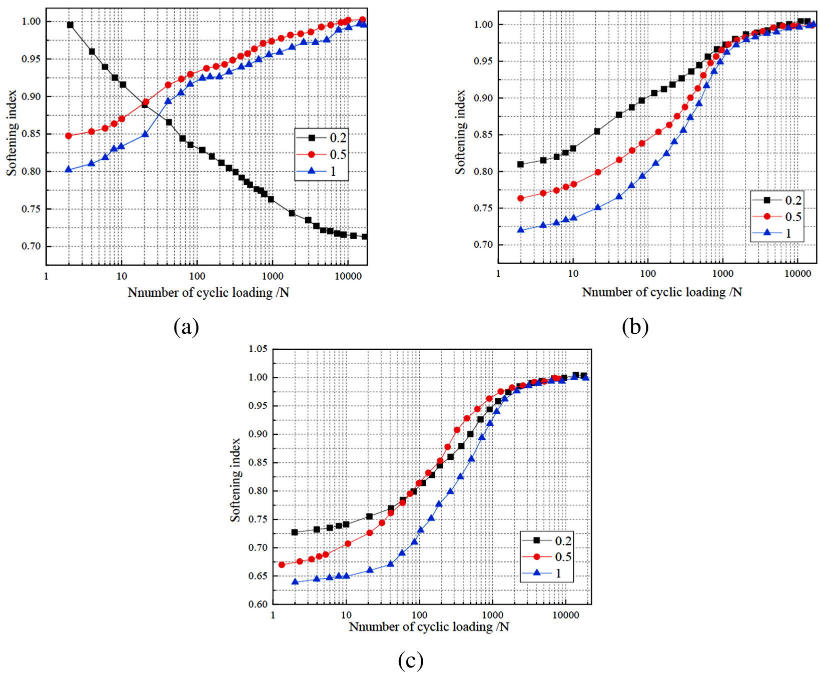

Fig. 11. Variation of soil stiffness for different radial cyclic stress ratios; (a) 150 kPa effective confining pressure, (b) 200 kPa effective confining pressure, (c) 250 kPa effective confining pressure

4.3. The effect of effective consolidation confining pressure ratio on the stiffness of freeze-thawing soft soil

Fig. 12. shows soil stiffness increases with higher effective confining pressure under a fixed radial cyclic stress ratio. When effective confining pressure rises from 200 kPa to 250 kPa, the softening index decreases by 12.5%, with an 18% reduction observed between 150 kPa and

250 kPa. Each 50 kPa increment reduces the softening index by approximately 15%. Higher radial cyclic stress ratios enhance soil compaction through vibrational loading, while the effect of confining pressure increments on stiffness changes diminishes progressively.

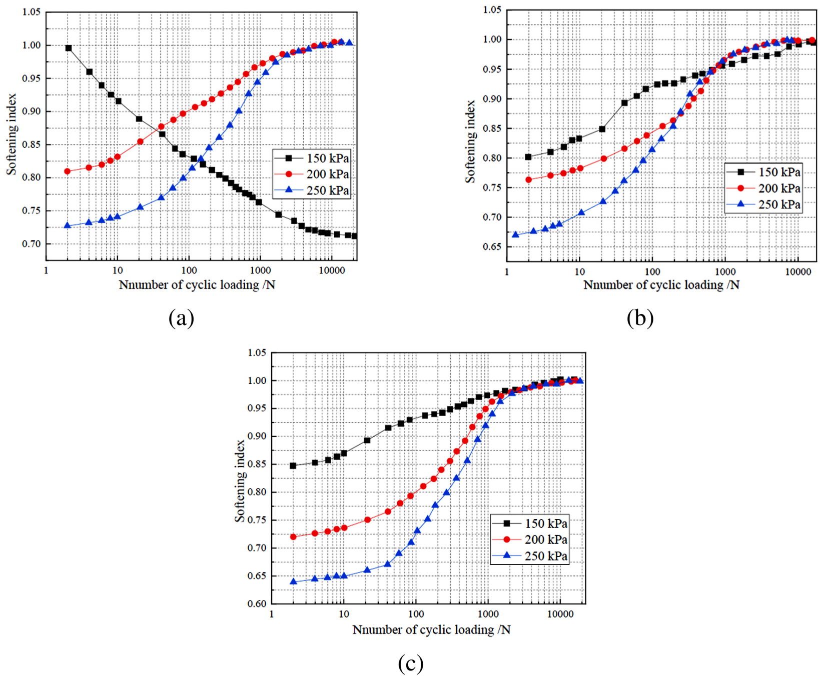

Fig. 12. Variation of soil stiffness under different effective consolidation confining pressures; (a) 0.2 Radial cyclic stress ratio, (b) 0.5 radial cyclic stress ratio, (c) 1 Radial cyclic stress ratio

Test results demonstrate that under low axial dynamic stress, artificial freeze-thawed soil transitions from softening to hardening stiffness behavior during bidirectional cyclic loading with increasing radial stress ratio and effective confining pressure [24]. Stiffness development curve analysis reveals that within the hardening range, increases in both parameters enhance soil hardening, though growth of either parameter limits the other's influence on stiffness.

4.4. The relationship between the hole pressure limit value and the stiffness hardening degree

The method by which freeze-thaw cycles weaken soft soil is closely linked to pore pressure levels. The pore pressure limit value reflects the densification of microscopic pores in soil under cyclic loading, while soil stiffness, influenced by sample density, indicates elastic deformation resistance. An increase in the pore pressure limit correlates with enhanced soil stiffness, modulated by soil structure. As shown in Fig. 13, elevated effective confining pressure shifts the pore pressure-stiffness relationship curve upward. After loading, the pore pressure limit increases, exhibiting a linear relationship with stiffness in freeze-thawed soft soil.

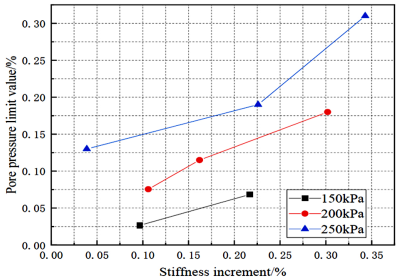

Fig. 13. Pore pressure-stiffness curve

5. Conclusions

1. Bidirectional cyclic loading enlarges soil pore pressure fluctuation amplitude compared to unidirectional cyclic loading, but residual pore pressure accumulation per cycle is not obvious. Under bidirectional loading, real-time soil pore pressure is mainly influenced by horizontal cyclic confining pressure, as axial loading and cyclic confining pressure align in frequency and phase.
2. Under identical test conditions, stabilizing cumulative pore pressure in freeze-thawed soil is more challenging compared to unfrozen soil. Freeze- thawed soil particles tend to break down and reorganize under cyclic loading, increasing water pressure in the soil and resulting in higher dynamic pore pressure in thawed soil than in unfrozen soil.
3. The pore pressure accumulation of freeze-thawed soft soil under bidirectional cyclic loading has three stages: rapid growth, slow growth and gradual stabilization. When the radial cyclic stress ratio reaches a certain value, the consolidation confining pressure and residual pore pressure of the soil body increase with the overburden thickness. At constant effective consolidation confining pressure of the soil body, the residual pore pressure rises with the radial cyclic stress ratio. An improved model for pore pressure development, considering effective confining pressure and radial stress ratio changes, is proposed. It simulates the pore pressure development of freeze-thaw soft soil under cross-river loading more accurately.
4. When the stress level exceeds a certain value, the soil stiffness turns hardening-type. For such specimens, as the radial stress ratio and effective confining pressure rise, the soil body's stiffness increases with closer soil particles. After the soil structure is compacted, a linear relationship exists between the soil pore pressure limit and the stiffness increase.

Acknowledgements

This research was supported by the Natural Science Foundation of Zhejiang Province (No.LQ24A020015), National Natural Science Foundation of China (No. 42477185) and the Graduate Research Innovation Fund Zhejiang University of Science and Technology (2024yjskc08).

References

[1] Z. Ding, B. Kong, X. Wei, M. Zhang, B. Xu, and F. Zhao, "Laboratory Testing to Research the Micro-Structure and Dynamic Characteristics of Frozen-Thawed Marine Soft Soil", *Journal of Marine Science and Engineering*, vol. 7, no. 4, art. no. 85, 2019, doi: 10.3390/jmse7040085.

[2] Z.-D. Cui, Y.-Q. Tang, and X.-X. Yan, "Centrifuge modeling of land subsidence caused by the high-rise building group in the soft soil area", *Environmental Earth Sciences*, vol. 59, no. 8, pp. 1819–1826, 2010, doi: 10.1007/s12665-009-0163-9.

[3] F. Casini, A. Gens, S. Olivella, and G.M.B. Viggiani, "Artificial ground freezing of a volcanic ash: laboratory tests and modelling", *Environmental Geotechnics*, vol. 3, no. 3, pp. 141–154, 2015, doi: 10.1680/envgeo.14.00004.

[4] B. Kong, S.-H. He, Y. Tao, and J. Xia, "Pore Structure and Fractal Characteristics of Frozen-Thawed Soft Soil", *Fractal and Fractional*, vol. 6, no. 4, art. no. 183, 2022, doi: 10.3390/fractalfract6040183.

[5] Z. Ding, J. Zhuang, X. Wei, B. Kong, and S. Ma, "Experimental study of pore pressure model of soft clay under cross-river subway loading", *Chinese Journal of Rock Mechanics and Engineering*, vol. 39, pp. 3178–3187, 2020, doi: 10.13722/j.cnki.jrme.2019.0976.

[6] J. Zhou and Y. Tang, "Practical model of deformation prediction in soft clay after artificial ground freezing under subway low-level cyclic loading", *Tunnelling and Underground Space Technology*, vol. 76, pp. 30–42, 2018, doi: 10.1016/j.tust.2018.03.003.

[7] F. Liu, et al., "The effects of the principal stress direction on the deformation behavior of frozen silt clay under the cyclic loading", *Transportation Geotechnics*, vol. 37, art. no. 100870, 2022, doi: 10.1016/j.trgeo.2022.100870.

[8] Y. Yang, Y. Lai, and X. Chang, "Laboratory and theoretical investigations on the deformation and strength behaviors of artificial frozen soil", *Cold Regions Science and Technology*, vol. 64, no. 1, pp. 39–45, 2010, doi: 10.1016/j.coldregions.2010.07.003.

[9] Q.-F. Gao, M. Jrad, M. Hattab, J.-M. Fleureau, and L.I. Ameur, "Pore Morphology, Porosity, and Pore Size Distribution in Kaolinitic Remolded Clays under Triaxial Loading", *International Journal of Geomechanics*, vol. 20, no. 6, art. no. 04020057, 2020, doi: 10.1061/(ASCE)GM.1943-5622.0001682.

[10] Y. Fujikura, "Estimation of Permeability for Sand and Gravel Based on Pore- Size Distribution Model", *Journal of Materials in Civil Engineering*, vol. 31, no. 12, art. no. 04019289, 2019, doi: 10.1061/(ASCE)MT.1943-5533.0002945.

[11] Q.-F. Gao, D. Zhao, L. Zeng, and H. Dong, "A Pore Size Distribution-based Microscopic Model for Evaluating the Permeability of Clay", *KSCE Journal of Civil Engineering*, vol. 23, no. 12, pp. 5002–5011, 2019, doi: 10.1007/s12205-019-2219-z.

[12] Z. Zhong, H. Zou, X. Hu, and X. Liu, "Experimental Study on Stiffness Softening of Soil-Rock Mixture Backfill under Metro Train Cyclic Load", *Advances in Materials Science and Engineering*, vol. 2021, art. no. 3024490, 2021, doi: 10.1155/2021/3024490.

[13] C. Wang and Y. Chen, "Experimental study on deformation behavior of saturated soft clay under bidirectional cyclic loading", *China Civil Engineering Journal*, vol. 43, pp. 573–576, 2010, doi: 10.15951/j.tmgcxb.2010.s1.075.

[14] J. Liu, L. Wang, X. Zhang, P. Lai, and T. Li, "Experimental study on dynamic pore pressure characteristics of silty clay under variable confining pressure", *Journal of Experimental Mechanics*, vol. 33, no. 4, pp. 634–640, 2018.

[15] Y. Xiao and J. Wang, "Method of settlement calculation for underlying layer of soft soil composite foundation based on load transfer mechanism", *Archives of Civil Engineering*, vol. 70, no. 1, pp. 543–555, 2024, doi: 10.24425/ace.2024.148927.

[16] C. Dong, "Experimental study on the hydrodynamic characteristics of saturated soft clay under long-term cyclic load", Ph.D. thesis, 2018.

[17] N. Ye and B. Chen, "Dynamic strength and pore pressure property of marine deposit soft clay", *Rock and Soil Mechanics*, vol. 32, pp. 55–60, 2011, doi: 10.16285/j.rsm.2011.s1.009.

[18] Z. Ding, M. Zhang, X. Wei, Q. Hong, Y. Zheng, and X. Yu, " Study on pore pressure and microstructure of frozen and thawed soft soil under subway cyclic loading", *Chinese Journal of Rock Mechanics and Engineering*, vol. 35, pp. 2328–2336, 2016, doi: 10.13722/j.cnki.jrme.2015.1620.

[19] Y. Wang, Y. Tang, S. Liao, and R. Li, "Experimental of pore pressure of reinforced soft clay around tunnel under subway vibrational loading", *Journal of Jilin University: Earth Science*, vol. 41, pp. 188–194, 2011, doi: 10.13278/j.cnki.jjuese.2011.01.042.

[20] J. Wang, Y. Cai, and X. Li, "Cyclic softening-pore pressure generation model for overconsolidated clay under cyclic loading", *Rock and Soil Mechanics*, vol. 29, pp. 3217–3222, 2008, doi: 10.16285/j.rsm.2008.12.053.

[21] J. Zhu, Y. Hong, J. Yan, X. Gong, and H. Zhao, "Cyclic degradation of soft clay subjected to repeated wave loading and stress relief during tunnel driving through a seawall", *China Civil Engineering Journal*, vol. 51, no. 12, pp. 111–119+139, 2018, doi: 10.15951/j.tmgcxb.2018.12.009.

[22] X. Wei, T. Zhang, Z. Ding, J. Jiang, and S. Zhang, "Experimental study on stiffness change of saturated soft clay with different degrees of consolidation under cyclic loading", *Chinese Journal of Geotechnical Engineering*, vol. 35, pp. 675–679, 2013.

[23] T. Godlewski, "Evaluation of stiffness degradation curves from in situ tests in various soil types", *Archives of Civil Engineering*, vol. 64, no. 4/II, pp. 285–307, 2018, doi: 10.2478/ace-2018-0075.

[24] M. Jastrzębska, "The Influence of Selected Parameters on Cycling Process on Cohesive Soils Shear Characteristics at Small Strain", *Archives of Civil Engineering*, vol. 56, no. 1, pp. 89–107, 2010.

Received: 2024-12-15, Revised: 2025-03-13